

# **Daughtership Release Flight Dynamics of the Aerial Surveyor Hybrid Autonomous Aircraft**

Wesley M. DeBusk\*  
*Georgia Institute of Technology  
Atlanta, GA*

## **Abstract**

Autonomous aerial vehicles offer capabilities that could benefit civil disaster relief and emergency response missions. The Aerial Surveyor hybrid autonomous vehicle concept combines the extended range of a fixed wing aircraft 'mothership' with the surface interactive ability of small coaxial rotorcraft 'daughterships.' The Aerial Surveyor is foreseen to have application to disaster relief and emergency response missions, however, analysis has not yet been conducted into the flight dynamics of such a vehicle system. This paper analyzes the release and freefall dynamics of the daughterships. Rigid body simulation combined with simple rotor momentum theory is used to study the unique flight envelope seen by the vehicle upon release for the first time. Resulting data concludes that stable configurations exist and that in-flight release is a feasible method of daughtership deployment.

---

\* USRP Associate Intern, Aeromechanics  
Branch, Flight Vehicle Research and Technology  
Division, Mail Stop 243-10, NASA Ames  
Research Center, Moffett Field, CA, 94035-  
1000.

Presented at the AHS Specialist's Conference on  
Aeromechanics, San Francisco, CA, Jan. 23-25,  
2008. Copyright 2008 by the American  
Helicopter Society International, Inc. All rights  
reserved.

## **Introduction**

Many civil or public service missions - particularly those related to disaster relief aerial surveillance - could benefit from the development and use of autonomous unmanned aerial vehicles (UAV). The need for disaster relief and emergency response (DRER) assets increases as the world population grows and urban expansion continues. The frequency and severity of natural disasters appear greater now than in the past<sup>2,3</sup>. Areas not readily accessible to conventional DRER efforts, whether because of remoteness and/or lack of road and airfield access, can quickly be affected by disasters of local origin (e.g. a tornado) and distant origin (e.g. a tsunami). Additionally, worldwide awareness of such incidences is increasing, yet availability of non-military DRER assets is limited.

Rotorcraft (here primarily helicopters) provide substantial flexibility in the role of DRER in that they are surface interactive aerial assets, i.e. in addition to the ability to fly considerable distances in short periods of time the vehicle has the short-field, or vertical, take off and landing (VTOL) capacity to allow for a significant ground-based mission component. This interactive ability allows for aerial distribution of high-value supplies, search and rescue assistance, rapid-response communications, and terrain surveys and exploration.

## **Aerial Surveyor**

The Aerial Surveyor is a hybrid autonomous vehicle concept that combines the range and endurance of a flying-wing aircraft with the surface interactive ability of small coaxial rotorcraft drones. A suite of system-of-systems autonomous hybrid vehicles has been previously proposed<sup>1,4,5</sup>, including specifically the Aerial Surveyor concept. In particular these aerial platforms might be optimally suited for DRER missions.

## **The Vehicle**

The Aerial Surveyor concept is comprised of two vehicle components: the flying wing 'mothership' and the coaxial rotorcraft drone 'daughterships.' The mothership's primary

role is to transport the drones over long range to wherever they are needed. An aircraft configuration offers range, endurance, and altitude capabilities beyond what is currently obtainable by rotorcraft platforms. The mothership will carry several drones externally, attached at points under the main wing body, as shown in Figure 1. Overall (combined) vehicle propulsion will be provided by the collective output of the individual drones themselves, each with two coaxial proprotors. Such a propulsion approach has also been subject of recent research into alternative VTOL UAV's in the form of tailsitter configurations<sup>6</sup>.

The Aerial Surveyor drone daughterships are the focus of this paper's study. The drones act as both a propulsion module for the mothership (in a collective sense) and, when aurally deployed/separated from the mothership, also acts as completely independent small rotorcraft capable of carrying sensor and communication equipment or even light cargo loads. To suit this dual duty operation, the drones will have a coaxial proprotor configuration. Proprotors are essentially adjustable pitch propellers with a wide range of collective and cyclic pitch travel, allowing for efficient hover as well as efficient high-speed flight. Figure 2 shows various dual-rotor configuration rotorcraft, including the XV-15, a precursor to the widely recognized V-22 Osprey aircraft, which utilizes proprotors<sup>7</sup>.

Proprotors are rigid in plane and, therefore, generate significant blade-root moments when flown in edgewise flight. These moments must be counteracted to maintain stability and controllability, therefore, two counter-rotating proprotors are used. To date, only side-by-side proprotor arrangements, i.e. tiltrotor aircraft, have been successfully flown. The physical layout of the two proprotors on the individual drones would conceivably be of one of two possible arrangements, each shown in Figure 3. The first possibility is to have both rotors close together offset above the drone body and center-of-gravity (CG). A second possibility is to have one rotor above and the other rotor below the drone body, nesting or sandwiching the rotors about the drone CG. Both configurations will be analyzed in this paper.

## ***Mission Profile***

A notional Aerial Surveyor mission can be described whereby the mothership vehicle serves as the means of conveyance by which to deliver individual surface-interactive rotary-wing drones to needed locations. The mothership will perform a CTOL (conventional take-off and landing) *fixed-wing* aircraft takeoff and cruise to a remote site, where it will either deploy one or more drones immediately, or loiter until the drones are needed. After deployment of all drones, or when all allotted fuel/energy is expended, the mothership will return to base. Each drone, when deployed, would complete a given individual and/or coordinated mission, then land, to be recovered later. This mission profile is depicted in Figure 4.

## ***Phases of Operation***

Four phases of operation exist in the notional mission of the Aerial Surveyor. Figure 5 demonstrates the sequence of these phases. The first two phases characterize the mothership operation. In the 'cruise' phase, the mothership with a full compliment of drones will takeoff and climb to altitude, then fly to a target zone. Depending on the timely need for drones on station at the target, the cruise phase can be conducted at conditions for maximum speed or endurance. After deployment of one or more drones, the mothership will be in the 'light cruise' phase. It may be desirable to maintain symmetry on the mothership by releasing drones only in pairs, however, in scenarios where more than one drone is unnecessary, it would also be possible to release a single drone, and adjust the throttle settings on the remaining drones to keep the mothership in trim.

The remaining two phases of operation characterize the drones. The 'release' phase describes the free motion of the drone between physical release from the mothership and steady state freefall. Analysis of the release phase is the focus of this paper. The final phase is the drone 'hover' phase in which the drone's control system becomes active and the drone transitions from freefall to controlled flight. After achieving a controllable flight, the drone will autonomously complete its tasked mission.

## ***Comparison With Conventional Systems***

Manned helicopters, aside from ground resources, are the primary conventional aerial DRER solution. Many issues arise when attempting to utilize manned helicopters in modern society. It can often be difficult to obtain approval to conduct manned flights in all areas, especially when operated by military forces. Larger aircraft can also disturb the surrounding areas when they fly, since full-scale helicopters generate significant noise, downwash, and vibrations. This can be dangerous to those on the ground when conducting flights over unstable terrain and/or structures remaining in the wake of a disaster.

Limited flight time also restricts the benefits of manned helicopter flights. A platform such as Aerial Surveyor can achieve longer loiter times by utilizing the fixed wing configuration. Additionally, Aerial Surveyor carries multiple drones, offering more assets, and an intrinsically greater area of coverage. Manned fixed wing platforms can obtain long loiter times, but surface interaction is more difficult. Parachute operations from manned fixed wing platforms could perform missions of similar nature, though they would be logistically challenging.

Flight of the Aerial Surveyor will be completely autonomous. Such robotic systems are often seen as lacking human perception. There will, however, be human controllers on the ground, at the vehicle's home base, able to issue commands to the vehicle or interact in whatever ways necessary. The true eyes and ears of the vehicle will be from these human controllers, who will now be able to watch and react without the demand of flying.

The value of unique aerial assets such as Aerial Surveyor may very well result from its non-military nature. Too often are DRER efforts military based, simply because there are insufficient civil resources. Robotic assets may be just as cost effective and efficient, and could serve to provide DRER assistance anywhere in the world, irrespective of social or political concerns.

## **Objective**

The purpose of this paper is to analyze the flight dynamics and stability of the Aerial

Surveyor daughterships. Such analysis must be performed to show that deployment of a coaxial proprotor configuration is possible via airdrop. Although only simple theory will be implemented here, a new set of assumptions will be used to accommodate the expected flight envelope. The combination of the specialized daughtership configuration with multiple phases of flight, including rotorcraft in high decent rates, creates a unique scenario, which will be analyzed in depth for the first time.

## **Daughtership Release Flight Dynamics**

### ***Approach***

A rigid body simulation<sup>8,18</sup>, implemented in MATLAB, is created here to study the flight dynamics of the Aerial Surveyor drone daughterships in freefall after release. Three degrees of freedom in two dimensions are allowed. Various levels of complexity are built into the simulation, and each level can be toggled, to give the user flexibility when looking at effects of design or flight control changes. At the basic level, only aerodynamic drag and gravity are included. The next step up in complexity adds all aerodynamic forces (lift, drag, and moments) to the model. Finally, the rotors are modeled as actuator disks and variable thrust is allowed. The simulation is built in modules (outlined in Figure 6), to allow for input and output routines to be developed independently of the core simulation code. This approach allows for greater flexibility when analyzing multiple vehicle configurations (Figure 7), as well as expandability for future projects.

Rotorcraft experience forces and moments that act in all three spatial dimensions and therefore generally require analysis in three dimensions. Coaxial configurations lessen the need for three-dimensional analysis, since moments produced on one rotor are balanced by a similar and opposite moment that would be produced on the other rotor at the same time. This is one reason a two dimensional simulation was chosen over a three dimensional simulation. Using only two spatial dimensions reduces the mathematical complexity, thus allowing for more detailed concentration on accurately modeling the unique flight regimes that are to be analyzed. Also, the lower level of mathematical complexity means that runtimes are faster. Given limited

time and computing power this is beneficial since more cases can be run and a broader understanding this dynamic problem can be obtained. Equation 1 gives the generalized differential equations of motion for a rigid body, which can be applied to either two or three dimensions.

The aerodynamic forces (lift and drag) model represents the vehicle as spherical and cylindrical bluff bodies, and the rotor blades as flat plates. Two dimensional, steady, incompressible flow is assumed, as this is an entirely low-subsonic problem<sup>9</sup>. Equations 2 and 3 compute lift and drag for incompressible flow.

Rotor effects are modeled using momentum theory<sup>10,11,12,13</sup>. Using momentum theory approach the rotors are replaced by actuator disks, which are assumed, for first-order analysis purposes, to experience uniform inflow. A figure of merit is nominally chosen to be 60%, reflecting efficiencies of similar configurations<sup>6</sup>. Thrust is calculated at each time step based on the current power output, induced velocity, and inflow conditions. Equations 4-6 are the momentum theory equations used for these thrust calculations. This method can predict vortex ring and autorotation states by categorizing the resulting induced velocity at each time step. This model, however, is limited in that it does not perform blade-element analysis, and therefore cannot predict some values and phenomena associated with this analysis such as advance ratio or un-powered autorotation. An implication of this is that the zero-power case used in simulation is equivalent to a fixed or braked rotor case, in which the rotor blades are not allowed to travel around the azimuth and become merely drag-producing structures.

### ***Code Validation***

The concept of simulating the effects of rotors on freefalling vehicles has been widely studied<sup>15,16,17</sup>. This analysis, however, is unlike past studies in that it combines a unique configuration with a unique flight envelope. Because this problem is different in these ways, it is necessary to check that the analysis satisfies fundamental boundary conditions. To provide validation for the physics models in this simulation the set of boundary conditions listed in Table 2 will be run and checked for the expected results.

### ***Methodology***

A set of metrics must be defined to qualify and quantify simulation output. The goal of the simulation is to observe what configurations and sets of parameters lead to stable freefall conditions. Acceptable cases would be those that reach a steady state freefall condition with the vehicle in an upright position and with minimal oscillatory motion. It is also desirable to minimize steady state descent velocity, so that a hover state is more easily obtainable, both from structural and controls standpoints, especially when considering steady state upright descent will in most cases occur with both rotors in the windmill brake state.

Flight path angle, angle of attack, and pitch rate will be used to monitor vehicle orientation and oscillation. Settling time and damping ratio<sup>14</sup> will be defined to quantify the angular oscillations. Settling time will be defined by the time taken for the magnitude of angular oscillation to be damped down to within a specified percentage of the initial oscillations. In other words, settling time is the amount of time it takes the vehicle to stabilize in freefall. Damping ratio is a measure of the damping present in the system, or of how sharply the amplitude of oscillations decreases each cycle. Rotor collective pitch angle will be quoted with the term ‘prop pitch.’ Propeller pitch will be defined as the inflow velocity for which a given rotor will turn through the air like a screw and not produce thrust. Propellers at higher pitch velocities will produce thrust over a greater range of flight velocities while ones at lower pitch velocities will produce higher static thrust. Terminal velocity, altitude, and range, and steady state behavior will also be used to quantify performance.

To analyze the stability of the daughterships, various parameters will be varied in simulation. The vehicle CG location with respect to the vehicle center of pressure (CP), throttle setting, and prop pitch setting will be swept in the first set, to determine stable vehicle configurations. Another set will sweep initial release conditions to determine stable release points for a nominally stable vehicle configuration. Stable configurations will also be compared to the lower fidelity models (vehicle body only, no rotors), to analyze the effects of the rotor thrust on freefall behavior.

In addition to a vehicle stability analysis, simulations will also determine operational clearance margins between the daughtership's rotors and the mothership during in-flight release. This information will be essential in proving the practicality of the concept and in setting criteria for the design of vehicles that will separate cleanly.

### ***Analysis***

The analysis will begin with a drone configuration in which the vehicle CG is nested between the two rotors. The vehicle model is presented in Figure 8.

An initial release velocity of 45 m/s was used to simulate each case for two minutes (120 seconds) of freefall time. The resulting 10% settling times, damping ratios, maximum rotations, and terminal velocities are presented in Figure 9, for a fixed prop pitch of 100 m/s. Settling times tend to decrease as CG offset increases. It is clear that not all combinations of CG offset and throttle setting result in steady state behavior that settles to below 10%, as the dark red areas of the graph indicate those areas that do not settle out to 10% or less. Maximum rotation indicates those configurations that 'tumble' prior to stabilizing, with red areas being those that 'tumble.' The damping ratio does not yield any strong trends, however it can be seen that damping ratio increases slightly as throttle setting decreases. Terminal velocity decreases as throttle setting increases up to around 50% throttle. Beyond 50% throttle, terminal velocity decreases for high CG offsets, but increases for low CG offsets.

Further analysis of settling behavior is presented in Figure 10. The blue regions of the graph indicate combinations that exhibit minimal steady state oscillations. In addition to varying CG offset and throttle setting, prop pitch is also varied. It can be seen in Figure 11 that prop pitch effects vehicle behavior similarly to throttle setting. This is a sensible result, because both throttle setting and prop pitch control rotor thrust output.

Since overall settling times and terminal velocities can both be large, it may also be important to consider the altitude required for a given vehicle to achieve a stable fall. Altitude loss at the 10% settling time is shown in Figure

12. It should be noted that even for moderate settling times, a lot of altitude could be required before steady state is reached.

The analysis will now consider the drone configuration in which the vehicle CG is below both rotors. The vehicle model is presented in Figure 13. The same initial conditions were used. This vehicle configuration displays the same trends. Minor differences can be observed, however. Fewer combinations exhibit high settling percentages, tumble, or show 'noisy' damping ratio behavior. Overall this configuration seems to be marginally more stable, including a zone of stability at high throttle settings. Graphical results for this configuration are presented in Figures 14, 15, 16, and 17.

After analysis of each all resulting data from these simulation runs, one configuration is selected as a baseline model for the next set of simulation runs, which will vary the initial conditions and release point. The baseline selected is the offset-CG configuration vehicle with parameters given in Table 3. Values for mass, length, rotor diameter, and moment of inertia were based on values common to model-scale radio control rotorcraft of size approximate to the conceptualized Aerial Surveyor daughterships. Single case behavior for the above initial conditions is shown in Figure 18.

The initial conditions are now varied to test a range of release velocities and altitudes. Figure 19 presents resulting data from this set of simulations. Neither release altitude nor velocity greatly effect the overall vehicle stability, as noted by every case settling to under 1% of peak amplitude. A significant trend presented here is that damping ratio peaks at low release altitudes and moderate release velocities. It can also be seen that settling times improve as release velocity increases, a correlation attributed to the higher dynamic pressure on the vehicle at higher velocities.

Further analysis of the Aerial Surveyor concept daughterships looks not at the vehicle stability, but rather at the clearance distance between the rotors and the mothership. Figure 20 pictorially demonstrates the initial release of a drone of the offset-CG configuration. Since the daughterships are designed to swing upright when released and would likely be released with non-zero rotor momentum, there is a risk that

their rotors may impact the mothership as the drone falls away. Simulations were run to compute the propotor clearance distance from the mothership. These simulations assumed that the daughtership is fixed to the mothership via a pylon attaching the daughtership CG to the mothership quarter chord. Fixing the drone CG location eliminates the influence of CG offset in these simulations, however, it should be noted that altering the CG offset without altering the vehicle sizing may change the initial spacing between the prop disk and the mothership leading edge, thus effecting the prop clearance distance. The vehicle configuration outlined in Table 3 is used as the model. Throttle setting and flight velocity at release are varied, while prop pitch and release altitude are held constant at 80 m/s and 2000 m respectively.

Resulting data from this set of simulations indicates that the rotor does indeed strike the mothership in some scenarios. The zero clearance (red shaded) areas of Figure 21 show the conditions for which prop strikes occur. A free release of the daughtership is the simplest method, however, it would be possible to employ a spring-loaded deployment mechanism. Such a mechanism would impart some initial separation velocity to the daughterships so that the likelihood of a collision is reduced or eliminated. Figure 21 also presents data for 1 m/s and 2 m/s initial separation velocity cases. It can be seen from the figure that increasing the initial separation velocity increases the margin on tight clearances, however reduces the maximum achievable clearance distances. This effect results from the more rapid daughtership onset of rotation due to higher total velocity. In general, slower release velocities and higher throttle settings yield the greatest clearance margins.

## ***Discussion***

Analysis of multiple variations of two configurations and several release points have generated clear trends as to the parameters that effect the stability of the Aerial Surveyor daughterships. The trends observed are very similar for both configurations. Slight differences do exist, but for purposes of overall stability, either configuration has significant parametric regions for which the vehicle is stable. This gives a choice when in concept design, allowing for more flexibility when

designing and configuring the mothership and daughterships.

Other parameters, however, do impact vehicle stability to a great extent. CG offset has the most influence. To obtain reasonable aerodynamic damping and stability, the CG must be offset from the CP by at least 10% of the vehicle length. This baseline may vary depending on how stringent the design criteria are for a specific aircraft design or mission. Throttle setting and prop pitch, both of which directly control thrust output, also alter the stability of the vehicle. Although it was seen that certain specific vehicle configurations are stable at high thrust settings, in general, only low thrust settings (below 50% of the hover requirement) correlate to moderate freefall stability.

In practice, the results obtained here outline the following release methodology. First the mothership will establish straight and level flight, at an airspeed and altitude within a fairly loose tolerance (e.g. between 50 and 150 knots and between 1000 and 6000 meters). Power setting on daughtership to be released is reduced to idle, and prop pitch is decreased. Finally the daughtership is released and thrust levels of the remaining daughterships are adjusted to keep the mothership in trim. It is assumed that when attached to the mothership in forward flight, that the daughterships will be oriented such that the CG is behind the CP so that they will stabilize in an upright sense in freefall.

A further influence on daughtership configuration choice, beyond freefall stability, is separation clearance between the rotors and the mothership. It has been shown that for a given configuration, there are release conditions for which clearance margins are high, and for conditions of low margin, 'active release' methods can be used to obtain more suitable prop clearances. In general, altering vehicle geometry may be the key to guaranteeing suitable separation clearance under any release condition.

## **Further Work**

This paper provides a framework for analyzing Aerial Surveyor daughtership stability, however, it is preliminary in nature. Further work is needed to test and validate results presented here, with the ultimate goal being

completion of a full-scale prototype. The next steps to be taken in simulated flight are to more accurately model the rotors. Simple theory provides acceptable first-run results, however, the fidelity of the simulation models must be increased and greater computing power allotted to obtain detailed results and design parameters.

Wind tunnel tests are a natural next step. Scale models can be tested at various attitudes to generate data of use in validating the simulation codes. Release tests may also be conducted in larger tunnels for further validation and prototype testing. In flight tests of model scale vehicles will then be a final step before full-scale development.

### Conclusions

Initial freefall stability and vehicle release analysis show that it is possible to design a coaxial rotorcraft that can be deployed via airdrop that is consistent with the Aerial Surveyor concept mission profile. A vehicle that exhibits stable freefall behavior is obtained by selecting appropriate vehicle parameters while such a vehicle is safely deployed by releasing it under appropriate flight conditions. This analysis has provided key insight into the feasibility of the Aerial Surveyor daughtership theory, though more work is necessary to fully develop the concept.

### Acknowledgements

The author would like to acknowledge Eduardo Solis of NASA Ames Research Center for assisting in the creation of the graphics presented in this paper.

### References

- <sup>1</sup> Young, L. A., "Future Roles for Autonomous Vertical Lift in Disaster Relief and Emergency Response," AHS International Specialists' Meeting on Advanced Rotorcraft Technology and Life Saving Activity, Aichi, Japan, November 15-17, 2006.
- <sup>2</sup> Luongo, G., "Facing Natural Disasters: Forecast, Warnings, Public Awareness of Hazards," European Science Foundation

Workshop on Situated Risk, Birmingham, England, September 15-16, 2000.

- <sup>3</sup> de Freitas, C.R., "Perceived Change in Risk of Natural Disasters Caused by Global Warming," *Engineering World*, Vol. 13, No. 1, pp 36-39, 2003.

- <sup>4</sup> Young, L.A., et al, "Mars Rotorcraft: Possibilities, Limitations, and Implications For Human/Robotic Exploration," IEEE Aerospace Conference, Big Sky, MT, March 2005.

- <sup>5</sup> Young, L.A., et. al., "New Concepts and Perspectives on Micro-Rotorcraft and Small Autonomous Rotary-wing Vehicles," AIAA 20th Applied Aerodynamics Conference, St. Louis, MO, June 24-27, 2002.

- <sup>6</sup> Baldwin, G. D., "Preliminary Design Studies of a Mono Tiltrotor (MTR) with Demonstrations of Aerodynamic Wing Deployment," AHS International Specialists Meeting, Chandler, AZ, January 23-25, 2007.

- <sup>7</sup> Leishman, J. G. and Ananthan, S., "Aerodynamic Optimization of a Coaxial Proprotor," 62nd Annual National Forum of the American Helicopter Society, Phoenix, AZ, May 9-11, 2006.

- <sup>8</sup> Baraff, D., "An Introduction to Physically Based Modeling: Rigid Body Simulation I – Unconstrained Rigid Body Dynamics," Robotics Institute at Carnegie Mellon University, 1997.

- <sup>9</sup> Anderson, J.D., "Fundamentals of Aerodynamics," McGraw-Hill Higher Education, Burr Ridge, IL, 2001.

- <sup>10</sup> Gessow, A. and Myers, G.C., "Aerodynamics of the Helicopter," Frederick Ungar Publishing Co., New York, NY, 1952.

- <sup>11</sup> Seddon, J., "Basic Helicopter Aerodynamics," American Institute of Aeronautics and Astronautics, Washington DC, 1990.

- <sup>12</sup> Johnson, W., "Helicopter Theory," Princeton University Press, Princeton, NJ, 1980.

- <sup>13</sup> Houston, S. S., "Analysis of Rotorcraft Flight Dynamics in Autorotation,"

AIAA Journal of Guidance, Control and Dynamics, Vol. 25 No. 1, pp. 33-39, 2002.

<sup>14</sup> Ogata, K., "Modern Control Engineering," Prentice Hall, Upper Saddle River, NJ, 2002.

<sup>15</sup> Ham, N.D., "An Experimental and Theoretical Investigation of a Supersonic Rotating Decelerator," Journal of the American Helicopter Society, Vol. 8, No. 1, pp. 8-18, 1963.





<sup>16</sup> Costello, M. and Beyer, E., "Performance of a Projectile/Rotor Kinetic Energy Reduction System," AHS International Specialists' Meeting, Chandler, AZ, January 23-25, 2007.

<sup>17</sup> Levine, A.D., et al., "An Analytical Investigation of the Aerodynamic and Performance Characteristics of an Un-powered Rotor Entry Vehicle," Document D-4537, National Aeronautics and Space Administration library, Washington, D.C. 1968.

<sup>18</sup> Condon, E.U. and Odishaw, H., et. al., "Handbook of Physics," McGraw-Hill Inc., New York, NY, 1967.

## Tables

**Table 1:** Comparison of DRER assets (Image source: Austrian Ministry of Defense, U.S. Army, and U.S. Coast Guard)

Asset Type	Advantages	Disadvantages	Civil or Military?
Conventional Ground 	Familiar, virtually no fuel/range/time limitations, numerous configurations	Slow, easily impeded by rough terrain	Both
Conventional Manned Fixed Wing 	Long range and loiter capability, large cargo capacity	Requires airfield, approval for international flights must be obtained	Military
Conventional Manned Helicopter 	Hover capability, can access most terrain, moderate cargo capacity	Limited range and endurance, approval for international flights must be obtained	Military
Aerial Surveyor Concept 	Long range, hover capability, large coverage area	Slower than manned aircraft, minimal cargo capacity, unfamiliar	Civil

**Table 2:** Code validation boundary conditions and test results

Test Condition	Result	As Expected?
All drag coefficients set to zero (no drag)	Trajectory matches free motion trajectory	Yes
Radially symmetric vehicle model	No rotation	Yes
Upright vehicle at 100% hover throttle setting	Vehicle hovers, no motion	Yes

**Table 3:** Parameters of a vehicle exhibiting stable behavior in freefall

Configuration	CG offset from both rotors
Mass	4.37 kg
Moment of Inertia	0.4133 kg m <sup>2</sup>
Length	0.9 m
Rotor Diameter	0.6 m
CG Offset from CP	0.2 m
Throttle Setting	20% of hover setting
Prop Pitch Setting	80 m/s

## Equations

$$\frac{d}{dt}\mathbf{Y}(t) = \frac{d}{dt} \begin{pmatrix} x(t) \\ R(t) \\ P(t) \\ L(t) \end{pmatrix} = \begin{pmatrix} v(t) \\ \omega(t)^* R(t) \\ F(t) \\ \tau(t) \end{pmatrix}$$

Eq. 1.

$$L = \frac{1}{2} \rho V^2 S C_L$$

$$D = \frac{1}{2} \rho V^2 S C_D$$

Eqs. 2-3.

$$T = \frac{P}{V \sin \alpha + v}$$

$$v_h = \sqrt{\frac{T}{2\rho A}}$$

$$v = \frac{v_h}{\sqrt{(V \cos \alpha)^2 + (V \sin \alpha + v)^2}}$$

Eqs. 4-6.

$$\zeta = \frac{\left(\frac{1}{n-1}\right) \ln\left(\frac{x_1}{x_n}\right)}{\sqrt{4\pi^2 + \left[\left(\frac{1}{n-1}\right) \ln\left(\frac{x_1}{x_n}\right)\right]^2}}$$

$$t_s = \frac{C_{\sigma_c}}{\zeta \omega_n}$$

Eqs. 7-8.



## Figures

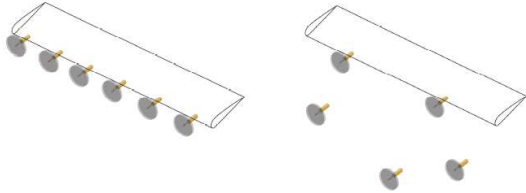


**Fig. 1:** Aerial Surveyor mothership and daughterships



**Fig. 2:** Examples of proprotor and coaxial rotorcraft

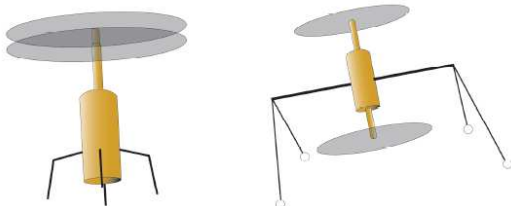


**Fig. 3:** Two possible daughtership configurations: both rotors offset above the vehicle body (left) and vehicle body nested between the rotors (right).

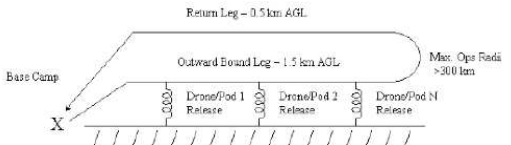


**Fig. 4:** Aerial Surveyor concept notional mission profile

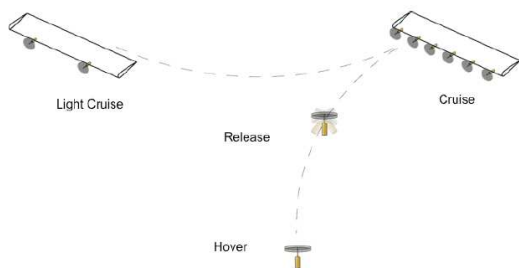


**Fig. 5:** Aerial Surveyor concept phases of operation

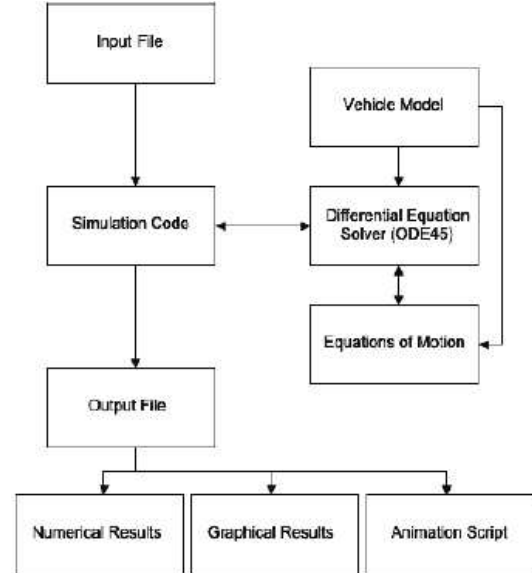


**Fig. 6:** Rigid body simulation flowchart

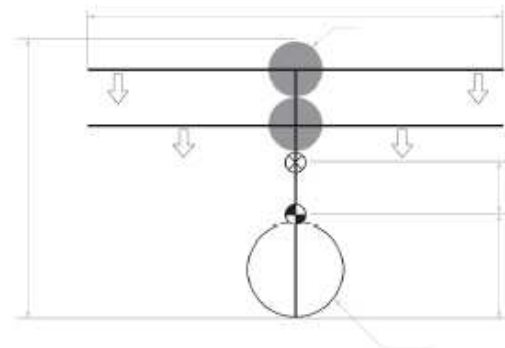


**Fig. 7:** Sample vehicle model definition for a coaxial helicopter drone

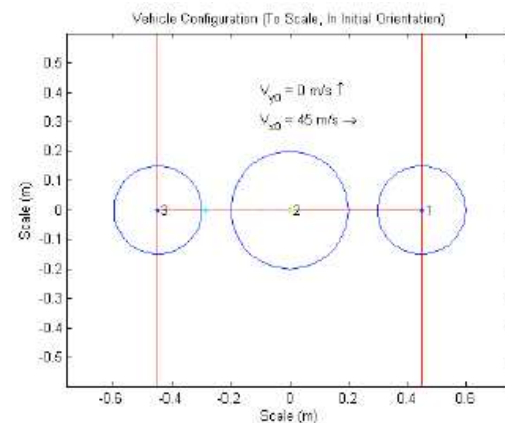


**Fig. 8:** Vehicle model for nested CG configuration

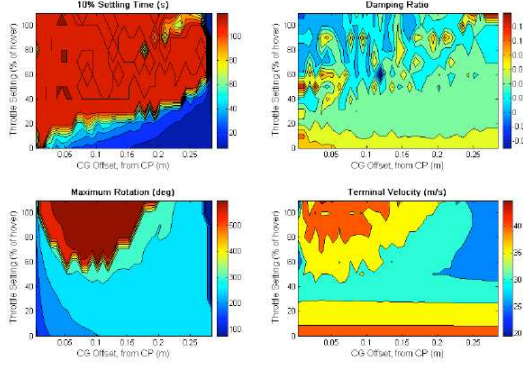


**Fig. 9:** Settling time, damping ratio, maximum rotation, and terminal velocity as functions of CG offset and throttle setting for nested CG configuration

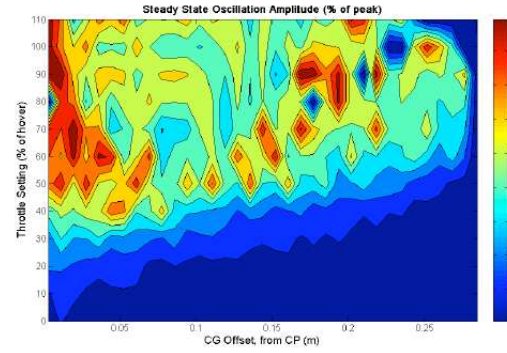


**Fig. 10:** Settling percentage as a function of CG offset and throttle setting for the nested CG configuration

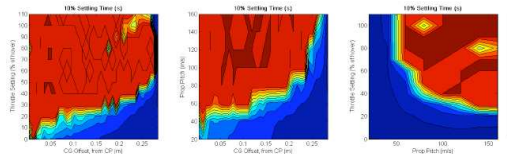


**Fig. 11:** Settling time as a function of all combinations of CG offset, throttle setting, and prop pitch for the nested CG configuration

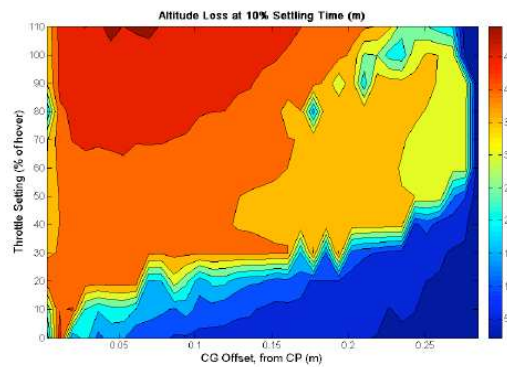


**Fig. 12:** Altitude loss at 10% settling time as a function of CG offset and throttle setting for the nested CG configuration

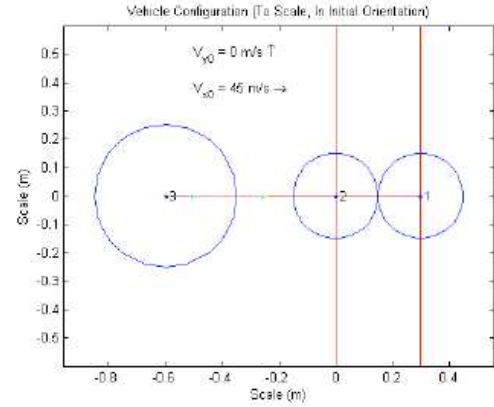


**Fig. 13:** Vehicle model for offset CG configuration

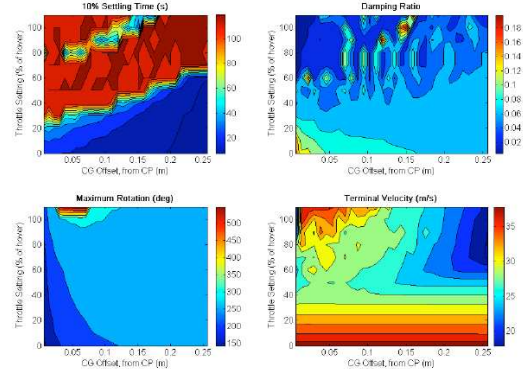


**Fig. 14:** Settling time, damping ratio, maximum rotation, and terminal velocity as functions of CG offset and throttle setting for the offset CG configuration

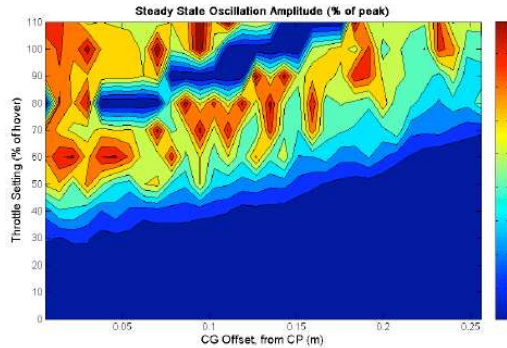


**Fig. 15:** Settling percentage as a function of CG offset and throttle setting for the offset CG configuration

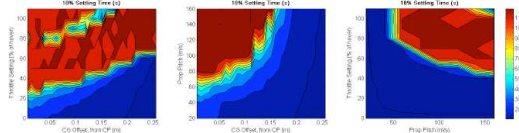


**Fig. 16:** Settling time as a function of all combinations of CG offset, throttle setting, and prop pitch for the offset CG configuration

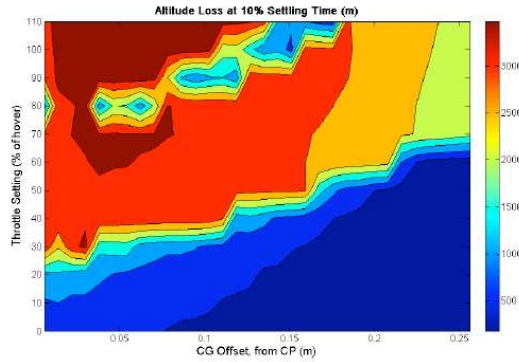


**Fig. 17:** Altitude loss at 10% settling time as a function of CG offset and throttle setting for the offset CG configuration

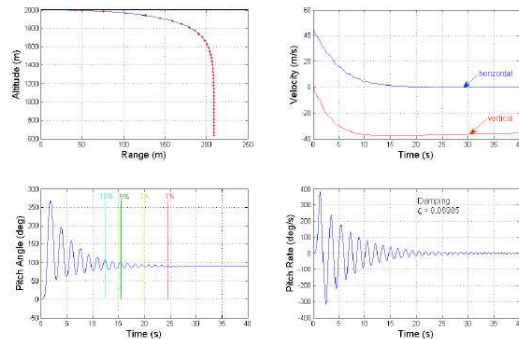


**Fig. 18:** Single case behavior for offset CG configuration with parameters as specified in Table 3

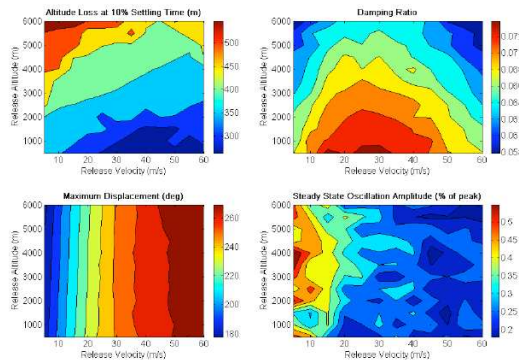


**Fig. 19:** Altitude loss at 10% settling time, damping ratio, maximum displacement, and steady state oscillation amplitude as functions of

release altitude and velocity for a known stable configuration

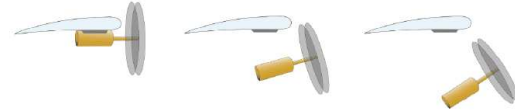


**Fig. 20:** Depiction of initial vehicle separation

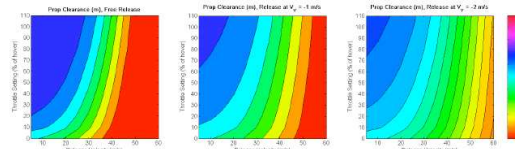


**Fig. 21:** Minimum prop clearance at release as a function of throttle setting and forward release velocity for a stable offset-CG configuration in a free release and releases at forced downward velocities of one and two meters per second